Mantle upwelling beneath the Tibetan Plateau based on P-wave teleseismic tomography

Chuansong He[1*]

[1]*Institute of Geophysics, CEA, Beijing 100081, China*

Abstract

I carried out P-wave teleseismic tomography and constructed the velocity structure of the upper mantle in the Tibetan Plateau based on the 58999 P-wave arrivals extracted from 2009 teleseismic events recorded by 721 temporary and 173 permanent seismic stations. A mushroom-shaped large-scale low-velocity anomaly, which might be associated with the mantle upwelling, is revealed. The mantle upwelling provides more heat to the base of the crust, which leads to a more ductile or more easily deformable lower crust, whereas the three large-scale low-velocity structures cover almost the entire area of the 80 km depth section, which implies that a rigid lithosphere is absent. In this situation, during the northward movement and subduction of the Indian plate, the ductile lower crust above the hot upper mantle facilitated crustal deformation and thickened, which led to the uplift of the Tibetan Plateau.

Key words: Mantle upwelling, Tibetan Plateau, delamination, subducted slab, P-wave teleseismic tomography.

Plain Language Summary

New P-wave teleseismic tomographies have been carried out in the Tibetan Plateau. The largest amount of data is used to construct the velocity structure of the upper mantle. Results revealed a mushroom-shaped large-scale low-velocity anomaly, which might be associated with the mantle upwelling. The mantle upwelling provides more heat to the base of the crust, which leads to a more ductile or more easily deformable lower crust. In this situation, during the northward movement and subduction of the Indian plate, the ductile lower crust above the hot upper mantle facilitated crustal deformation and thickened, which led to the uplift of the Tibetan Plateau.

1. Introduction

The Tibetan Plateau constitutes the highest and largest continental plateau on Earth. The current size, shape and height of the plateau are considered to have resulted from the collision of the Eurasian plate and the Indian plate over the past 70-50 Ma (e.g., Dewey et al., 1988; Yin & Harrison, 2000; Hetzel, 2013; Li et al., 2018; Xiao et al., 2020). However, the role of this collision in the growth of the Tibetan Plateau remains debated (Zhu et al., 2009; Liu et al., 2010).

Various models have been suggested to elucidate the deformation (crustal thickening) and uplift of the Tibetan Plateau, including the following: (1) lateral

[1*] Corresponding author: Chuansong He (hechuansong@aliyun.com)

extrusion of thickened blocks along strike-slip faults (e.g., Molnar & Tapponnier, 1975; Tapponnier et al., 2001), (2) lower crustal channel flow (Royden et al., 2008), and (3) lithospheric thickening in southern Asia induced by thrust faulting (Dewey & Burke, 1973; Toksoz & Bird, 1977). In particular, receiver function (Kind & Yuan, 2002, 2010, Kosarev et al., 1999, Kumar et al., 2006; Zhao et al., 2010), magnetotelluric and surface wave dispersion data (Vozar et al., 2014) and teleseismic P- and S-wave tomography indicated subhorizontal underthrusting of the Indian lithosphere beneath the Tibetan Plateau ranging from 100 to 200 km, which led to the crustal thickening or uplift of the Tibetan Plateau.

However, recent geophysical studies have provided new evidence that challenges certain notions; for example, numerical modelling has indicated that subducted slab or lithosphere is retained for only tens of millions of years in the mantle (Burkett & Gurnis, 2012), and a receiver function analysis (He et al., 2015) has revealed a felsic lower crust induced by lower crustal/lithospheric delamination in Tibet, which implies that it cannot be assumed that the crust was thickened by subhorizontal underthrusting of the Indian lithosphere beneath the Asian continent.

Alternately, regional tomography studies (e.g., Liang et al., 2016; Nunn et al., 2014) and large region surface wave tomography (e.g., Li et al., 2013, Chen et al., 2017) have revealed significant low-velocity anomalies in the upper mantle of the Tibetan Plateau, which may be associated with its uplift. However, due to the limitation of the regional velocity model and the lateral resolution of the surface velocity model, the scale and shape of the low-velocity anomalies are still unclear. In this study, I collected data recorded by temporary and permanent seismic stations to perform detailed teleseismic P-wave tomography in the entire Tibetan Plateau (Fig. 1) to reconstruct the velocity structure and evaluate the dynamical process.

1. **Results**

Three large-scale low-velocity perturbations (Lv1, Lv2 and Lv3) appear at 80, 100, 200 and 300 km depth (Fig. 2). Lv1 and Lv2 are located in the north-central part of Tibet, and Lv3 is located in the southern part. Lv4 appears at depths of 400, 500, 600 and 700 km. Li et al. (2006) and Li Y.H. et al. (2013) also identified a similar large-scale low-velocity structure at a 100-300 km depth based on P-wave of Southeast Asia and Rayleigh wave tomography of East Asia. Liang et al. (2016) determined a large-scale low-velocity structure using body-wave finite-frequency tomography at a depth of 84-253 km at the south and central part of the Tibetan Plateau. Pandey et al. (2014) also defined a large low-velocity region at a depth of 100 km in this area using the Rayleigh wave tomography of China and the surrounding regions. Recently, S-wave velocity models have also identified a large low-velocity structure at depths of 80 km and 130 km under the centre of the Tibetan Plateau (Chen et al., 2017; Li & Song, 2018).

At a depth of 80 km, Hv1 appears in the southern part of the Tibetan Plateau, whereas the surface wave dispersion analysis indicates that the high-velocity anomalies cover all southern parts of the Tibetan Plateau (Agius, & Lebedev, 2013). I consider that it may be induced by the lateral resolution difference between the surface wave technique and the teleseismic P-wave tomography. Hv2 appears at a depth of 200-500 km. Hv3 is at a depth of 600-700 km. In this study, I also extract P-wave velocity images (Fig. S6), which are consistent with the images of the P-wave velocity perturbation. Major low velocity and high velocity anomalies (Fig. 2, Fig. S6) located within a high resolution and ray density region (Fig. S2, Fig. S7).

To check the above results, five P-wave velocity perturbation profiles were created along the latitudinal direction (Fig. 3), and the results show that the Lv1 is located in the middle and northern part of Tibet (Fig. 3a, b and c), whereas Lv3 is located in the southern part of Tibet (Fig. 3a, b, c and d). Lv3 is connected with Lv4 (Fig. 3d). The slab-like high-velocity structures (Hv2, Hv3 and Hv6) appear at a depth range of 100-700 km (Fig. 3a, b, c and e). Hv4 and Hv5 appear at a depth of 500-600 km (Fig. 3b and c). Major low-velocity (Lv1-Lv4) and high-velocity (Hv1-Hv6) anomalies are located within the high-resolution and ray density region (Fig. S7, Fig. S8).

I also conducted four profiles along the longitudinal direction (Fig. 4). The results show that the large-scale low velocity anomaly (Lv1, Lv2) with mushroom-shape is nearly 1000 km long (Fig. 4g), whereas the Lv4 is the root of the Lv1 and Lv2 (Fig. 4g) and is located within the high resolution and ray density region (Fig. S7, Fig. S9). Additionally, I carried out synthetic tests along the 36°N and 34°N profiles (Fig. 5), and the results indicate that the major low-velocity anomaly (Lv1, Lv2 and Lv3) can be defined by this set of data (Fig. S10, Fig. S11). Another synthetic test indicates that the 200 km thick high-velocity anomaly can be determined by this set of data (Fig S12, 13).

1. **The high-velocity anomalies associated with break-off of the subducted slab and delamination**

In the Qiangtang terrane, the formation of Eocene–Oligocene alkaline volcanic rocks (50–26 Ma) (e.g., Ding et al., 2003; Williams et al., 2004) is correlated with the northward underthrusting of the Indian continental lithosphere (Guo et al., 2006) and the Lhasa continental lithosphere (Lai et al., 2007; Chi et al., 2005), together with the southward "continental underthrusting" of the Songpan-Ganzi Terrane (Roger et al., 2000; Ding et al., 2003). The tomographic results of Zhang et al. (2015) and Liang et al. (2016) showed that underthrusted Indian slab occurs beneath the central part of the Tibetan Plateau.

These processes might have resulted in the break-off of the subducted slab beneath the central part of the Tibetan Plateau (Wortel & Spakman, 1992; Hildebrand & Bowring, 1999; Davies & von Blanckenburg, 1995; Ferrari, 2004; Coulon et al., 2002; Chen et al., 2014). A break-off of the subducted lithosphere in the upper mantel has been revealed by a body-wave seismic tomography

in the India-Asia collision zone (Replumaz et al., 2013, 2014). Our results also show some subducted slab-like high-velocity anomalies in the upper mantle (Fig. 3, Hv2, Hv3 and Hv6), which may be detached fragments of subducted Indian and Asian lithosphere. Based on the location of Hv2, Hv3 and Hv6 and previous studies (Liang et al., 2012; Bao et al., 2012), we consider that Hv3 and Hv6 may belong to the Indian plate's lithosphere and were generated by the break-off of slab due to the northward subduction of the Indian plate (Bao et al., 2012); furthermore, Hv2 may belong to the European plate's lithosphere and was generated by the break-off of the southward subducted slab (Liang et al., 2012).

Large-scale delamination of the mantle lithosphere occurred at 8 to 12 Ma in the Tibetan Plateau (Turner et al., 1996; Molnar et al., 1993; Jiménez-Munt & Platt, 2006). The void formed by delamination is filled by the rising asthenosphere, and the hot upwelling triggers melting at the base of the lower crust and generates adakites (Jull & Kelemen, 2001), such as the Miocene adakite-like rocks in southern and northern Tibet (Chung et al., 2003; Ding et al., 2007). The low-velocity structure at a depth of 80 km and that almost covers the entire region of Tibet implies the absence or delamination of the rigid lithosphere and asthenospheric upwelling. Some high-velocity structures (Hv4 and Hv5) might be associated with the delamination of the lower mantle lithosphere, whereas other high-velocity structures (Hv2, Hv3 and Hv6) that may be related to the delamination of the lithosphere cannot be excluded.

1. **Mantle upwelling**

The magmatism in continent–continent collision zones results from mantle upwelling and mantle–crust interactions, which lead to the growth and reworking of the continental crust (Stern & Kilian, 1996; Castillo & Newhall, 2004; Bolhar et al., 2008; Sui et al., 2013). Lithospheric mantle delamination and the slab breakoff has been suggested as a major cause for the mantle upwelling in an active orogeny (Bird, 1979; Houseman et al., 1981; Kay & Kay, 1993; Davies & von Blanckenburg, 1995; Niu, 2017).

Furthermore, when a subducted slab breaks off or the lithosphere delaminates, the material sinks down and accumulates in the mantle transition zone (MTZ), where it forms so-called 'second continents' at the 660 km discontinuity (Lustrino, 2005; Kawai et al., 2013). The hydrous minerals linked with this debris serve as 'water tanks' that can induce dehydration melting; due to the buoyancy, the melting triggers vertical mantle flow or plume-like upwelling (Schmandt et al., 2014; Lustrino, 2005). Numerical simulations corroborated that the mantle (or plume-like) upwelling is mainly a mushroom-shaped low-velocity structure (David & Yuen, 2000; Wang et al., 2013; Cloetingh et al., 2013). Accordingly, I proposed that the mushroom shaped low-velocity anomaly (Fig. 4g) represents standard mantle upwelling, which might be induced by the break-off of a subducted slab combined with the delamination of the mantle lithosphere.

1. **Discussion**

Mantle upwelling can lead to basaltic magma invading into the crust, which generates high heat value and low velocity anomaly (zone) in the crust. The thermal structure of the continental lithosphere beneath China indicates that there is a distinctive anomaly of high-heat flow beneath the Tibetan Plateau at a depth of 20-80 km (Sun et al., 2013). A prominent low-velocity zone in the crust of certain areas of Tibet has been reported in a number of geophysical studies (Nelson et al., 1996; Alsdorf & Nelson, 1999; Yuan et al., 1997; Wei et al., 2001; Xu et al., 2011; Yang et al., 2012; Unsworth et al., 2004; Xu et al., 2015; Agius & Lebedev, 2014; 2017). These results corroborated the mantle upwelling beneath the Tibetan Plateau.

Tomography is the only tool available to detect the deep 3-D velocity structure of Earth, whereas isotope geochemistry can provide the time of mantle processes, or a fourth dimension. The results inferred from geochemistry and tomography can be combined to construct geological models of the mantle structure and dynamics (Foulger et al. 2013). The volumetrically small but widespread Cenozoic highly potassic volcanism on the Plateau(Zhao et al., 2009) might be related to the heat accumulation beneath the crust of Tibet (e.g., McKenzie & Priestley, 2016; Niu, 2017) generated by the mantle upwelling, which implies the mantle upwelling identified in this study occurred in the Cenozoic. Meanwhile, this kind of heat accumulation also led to the formation of the more ductile lower crust so that the crust of Tibet was easily deformed and thickened given the northward movement and subduction of the Indian Plate.

1. Conclusions

This study identified a mushroom-shaped large-scale low-velocity anomaly with a length of nearly 1000 km originating from the central part of the Tibetan Plateau (or Qiangtang terrane), and this anomaly extends across Tibet at a depth of 80 km (or at the top of the mantle). It might represent mantle upwelling, resulting from the break-off of subducted slabs and delamination of the mantle lithosphere in the Cenozoic. This structure provided enhanced heat to the base of the lower crust, making the lower crust more ductile and more easily deformed. This situation led to rapidly crustal thickening or uplift of the Tibetan Plateau due to the Cenozoic northward movement of the Indian plate.

Acknowledgements

I am grateful to the National K&D Plan of China (Grant No. 2017YFC601406). The data for this study can be accessed at https://doi.org/10.5281/zenodo.4505994. Tomography code was provided by Prof. D. Zhao.

References

Alsdorf, D., & Nelson, D. (1999). Tibetan satellitemagnetic low: evidence for widespread melt in the Tibetan crust?. *Geology,* 27, 943-946.

Agius, M. R., & Lebedev, S. (2013). Tibetan and Indian lithospheres in the upper mantle beneath Tibet: Evidence from broadband surface-wave dispersion. Geochemistry, Geophysics, Geosystems, 14(10), 4260-4281. https://doi:10.1002/ggge.20274

Agius, M. R., & Lebedev, S. (2014). Shear-velocity structure, radial anisotropy and dynamics of the Tibetan crust. *Geophys. J. Int.*, 199(3), 1395-1415. https://doi: 10.1093/gji/ggu326

Agius, M. R., & Lebedev, S. (2017). Complex, multi-layered azimuthal anisotropy beneath Tibet: evidence for co-existing channel flow and pure-shear crustal thickening. *Geophys. J. Int.*, 210(3), 1823-1844. https://doi:10.1093/gji/ggx266

Bao, X. Y., Sandvol, E., Chen, Y. J., Ni, J., Hearn, T., & Shen, Y. (2012). Azimuthal anisotropy of Lg attenuation in eastern Tibetan Plateau. *J. Geophys. Res.,* 117, B10309. https://doi.org/10.1029/2012JB009255

Bolhar, R., Weaver, S. D., Whitehouse, M. J., Palin, J. M., Woodhead, J. D., & Cole, J. W. (2008). Sources and evolution of arc magmas inferred fromcoupled O and Hf isotope systematics of plutonic zircons from the Cretaceous Separation Point Suite (New Zealand). *Earth Planet. Sc. Lett.,* 268, 312-324. https: //doi.org/10.1016/j.epsl.2008.01.022

Boschi, L., Becker, T., Soldati, G., & Dziewonski, A. M. (2006). On the relevance of Born theory in global seismic tomography. *Geophys. Res. Lett.,* 33, L06302. https://doi.org/10.1029/2005GL025063.

Bird, P. (1979). Continental delamination and the Colorado Plateau. *J. Geophys. Res.* 84, 7561-71. https://doi.org/10.1029/jb084ib13p07561

Burkett, E., & Gurnis, M. (2012). Stalled slab dynamics. *Lithosphere,* 5, 92-97. https://doi.org/10.1130/L249.1

Castillo, P. R., & Newhall, C. G. (2004). Geochemical constraints on possible subduction components in lavas of Mayon and Taal Volcanoes, southern Luzon, *Philippines. J. Petrol.,* 45, 1089-1108. https://doi.org/10.1093/petrology/egh005

Chen, M., Niu, F. L., Tromp, J., Lenardic, A., Lee, C. T. A., Cao, W., & Ribeiro, J. (2017). Lithospheric foundering and underthrusting imaged beneath Tibet. *Nat. Commun.,* 8, 15659. https://doi.org/10.1038/ncomms15659OI

Chen, Y., Zhu, D. C., Zhao, Z. D., Meng, F. Y., Wang, Q., Santosh, M., Wang, L. Q., Dong, G. C., & Mo, X. X. (2014). Slab breakoff triggered ca. 113 Ma magmatism around Xainza area of the Lhasa Terrane, Tibet. *Gondwana Res.,* 26, 449-463. https://doi.org/10.1016/j.gr.2013.06.005

Chi, X. G., Li, C., & Jin, W. (2005). Cenozoic volcanism and lithospheric tectonic evolution in Qiangtang area, northern Qinghai-Tibetan plateau. *Sci. China Ser. D,* 48. https://doi.org/1011-1024, 0.1007/s11430-007-0039-3

Chung, S. L., Liu, D., Ji, J., Chu, M. F., Lee, H. Y., Wen, D. J., Lo, C. H., Lee, T. Y., Qian, Q., & Zhang, Q. (2003). Adakites from continental collision zones: melting of thickened lower crust beneath southern Tibet. *Geology,* 31, 1021-1024. http://ntur.lib.ntu.edu.tw/handle/246246/172310

Cloetingh, S.,Burov, E., & Francois, T. (2013). Thermo-mechanical controls on intra-plate deformation and the role of plume-folding interactions in continental

topography. *Gondwana Res.,* 24, 815-837. https://doi.org/10.1016/j.gr.2012.11.012

Coulon, C., Megartsi, M., Fourcade, S., Maury, R., Bellon, H., Louni-Hacini, A., Cotton, J., Coutelle, A., & Hermitte, D. (2002). Post-collisional transition from calc-alkaline to alkaline volcanism during the Neogene in Oranie (Algeria): magmatic expression of a slab breakoff. *Lithos* 62, 87-110. https://doi.org/10.1016/S0024-4937(02)00109-3

David, B. D., & Yuen, A. (2000). Mantle plumes pinched in the transition zone. *Earth Planet. Sc. Lett.,* 178, 13-27. https://doi.org/10.1016/S0012-821X(00)00063-7

Davies, J. H., & von Blanckenburg, F. (1995). Slab breakoff: a model of lithosphere detachment and its test in the magmatism and deformation of collisional orogens. *Earth Planet. Sc. Lett.,* 129, 85-102. https://doi.org/10.1016/0012-821X(94)00237-S

Dewey, J. F., & Burke, K. C. A. (1973). Tibetan, Variscan, and Precambrian basement reactivation—products of continental collision. *J. Geol.,* 81, 683-692. http://dx.doi.org/10.1086/627920

Dewey, J. F., Shackleton, R. M., Chang, C. F., & Sun, Y. Y. (1988). The tectonic evolution of the Tibetan Plateau. Phil. Trans. *Roy. Soc. London. Series A,* 327, 379-413. https://doi.org/10.1098/rsta.1988.0135

Ding, L., Kapp, P., Yue, Y. H., & Lai, Q. Z. (2007). Post collisional calc-alkaline lavas and xenoliths from the southern Qiangtang terrane, central Tibet. *Earth Planet. Sc. Lett.,* 254, 28-38. https://doi.org/10.1016/j.epsl.2006.11.019

Ding, L., Kapp, P., Zhong, D., & Deng, W. (2003). Cenozoic volcanism in Tibet: evidence for a transition from oceanic to continental subduction. *J. Petrol.*, 44, 1833-1865. https://doi.org/10.1093/petrology/egg061

Eberhart-Phillips, D. (1986). Three-dimensional velocity structure in Northern California Coast Ranges from inversion of local earthquake arrival times. *Bull. Seismol. Soc. Am.,* 76, 1025-1052. https://doi.org/10.1029/JB095iB10p15343

Ferrari, L. (2004). Slab detachment control on mafic volcanic pulse and mantle heterogeneity in central Mexico. *Geology,* 32, 77-80. https://doi.org/10.1130/G19887.1

Foulger, G. R., Panza, G. F., Artemieva, I. M., Bastow, I. D., Cammarano, F., Evans, J. R., Hamilton, W. B., Julian, B. R., Lustrino, M., Thybo, H., & Yanovskaya, T. B. (2013). Caveats on tomographic images. *Terra Nova*, 25(4), 259-281. https://doi.org/doi: 10.1111/ter.12041

Guo, Z. F., Wilson, M., Liu, J. Q., & Mao, Q. (2006). Post-collisional, potassic and ultrapotassic magmatism of the Northern Tibetan plateau: constraints on characteristics of the mantle source, geodynamic setting and uplift mechanisms. *J. Petrol.,* 47, 1177-1220. https://doi.org/10.1093/petrology/egl007

Hansen, P. (1992). Analysis of discrete ill-posed problems by means of the L-curve. *SIAM Rev.,* 34, 561-580. https://doi.org/10.1137/1034115

He, C. S., Santosh, M., Dong, S. W., & Wang, X. C. (2015). Crustal thickening and uplift of the Tibetan Plateau inferred from receiver function analysis. *J. Asian Earth Sci.,* 99, 112-124. https://doi.org/10.1016/j.jseaes.2014.12.011

Hetzel, R. (2013). Active faulting, mountain growth, and erosion at the margins of the Tibetan Plateau constrained by in situ-produced cosmogenic nuclides. *Tectonophysics,* 582, 1-24. https://doi.org/10.1016/j.tecto.2012.10.027

Hildebrand, R. S., & Bowring, S. A. (1999). Crustal recycling by slab failure. *Geology,* 27, 11-14. https://doi.org/10.1130/0091-7613(1999)027<0011:CRBSF>2.3.CO;2

Houseman, G. A., McKenzie, D. P., & Molnar, P. (1981). Convective instability of a thickened boundary layer and its relevance for the thermal evolution of continental convergent belts. *J. Geophys. Res.,* 86, 6115-32.

Huang, W. C., Ni, J. F., Tilmann, F., Nelson, D., Guo, J., Zhao, W., Mechie, J., Kind, R., Saul, J., Rapine, R., & Hearn, T. M. (2000). Seismic polarization anisotropy beneath the central Tibetan Plateau. *J. Geophys. Res.*,105, 27979-27989. https://doi.org/10.1029/2000JB900339

Jiang, G. M., Zhang, G. B., Zhao, D., Lü, Q.T., Li, H. Y., & Li, X. F. (2015). Mantle dynamics and Cretaceous magmatism in east-central China: Insight from teleseismic tomograms. *Tectonophysics,* 664, 256-268. https://doi.org/10.1016/j.tecto.2015.09.019

Jiménez-Munt, I., & Platt, J. P. (2006). Influence of mantle dynamics on the topographic evolution of the Tibetan Plateau: results from numerical modelling. *Tectonics,* 25, TC6002. https://doi.org/10.1029/2006TC001963

Jull, M., & Kelemen, P. B. (2001). On the conditions for lower crustal convective instability. *J. Geophys. Res.,* 106, 6423-6446, https://doi.org/10.1029/2000JB900357

Kay, R. W., & Kay, S. M. (1993). Delamination and delamination magmatism. *Tectonophysics* 219, 177-189. https://doi.org/10.1016/0040-1951(93)90295-U

Kawai, K., Yamammoto, S., Tsuchiya, T., & Maruyama, S. (2013). The second continent: Existence of granitic continental materials around the bottom of the mantle transition zone. *Geosci. Front.,* 4, 1-6. https://doi.org/10.1016/j.gsf.2012.08.003

Kennett, B. L. N., & Engdahl, E. R. (1991). Travel times for global earthquake location and phase identification. *Geophys. J. Int.* 105, 429-465. https://doi.org/10.1111/j.1365-246X.1991.tb06724.x

Kind, R., & Yuan, X. (2010). Seismic images of the biggest crash on Earth. *Science*, 329(5998), 1479-1480. https://doi :10.1126/science.1191620

Kind, R., Yuan, X., Saul, J., Nelson, D., Sobolev, S. V., Mechie, J., Zhao, W., Kosarev, G. Ni, J., Achauer, U., & Jiang, M., (2002), Seismic im-

ages of crust and upper man- tle beneath Tibet: Evidence for Eurasian plate subduction, *Science*, 298(5596), 1219-1221. https://doi:10.1126/ science.1078115

Kosarev, G., Kind, R., Sobolev, S. V., Yuan, X., Hanka, W., & Oreshin, S. (1999). Seismic evidence for a detached India lithospheric mantle beneath Tibet. *Science,* 283, 1306-1309. https://doi.org/10.1126/science.283.5406.1306

Kumar, P., Yuan, X., Kind, R., & Ni J. (2006). Imaging the colliding Indian and Asian lithospheric plates beneath Tibet, *J. Geophys. Res.*, 111, B06308. https://doi:10.1029/2005JB003930

Lai, S. C., Qin, J. F., Li, Y. F., & Long, P. (2007). Geochemistry and Sr–Nd–Pb isotopic characteristics of theMugouriwang Cenozoic volcanic rocks from Tibetan Plateau: constraints onmantle source of the underplated basic magma. *Sci. China Ser. D,* 50, 984-994. https://doi.org/10.1007/s11430-007-0039-3

Laske, G., Masters, G., Ma, Z., & Pasyanos, M. E. (2012). CRUST1.0: an updated global model of Earth's Crust. *Geophys. Res. Abstr.,* 14 (EGU 2012-37431).

Lei, J. S., Zhao, D., Steinberger, B., Shen, F. L., & Li, Z. X. (2009). New seismic constraints on the upper mantle structure of the Hainan plume. *Phys. Earth Planet. In.,* 173, 33-50. https://doi.org/10.1016/j.pepi.2008.10.013

Li, C., van der Hilst, R. D., & Toksöz, M. N. (2006). Constraining P-wave velocity variations in the upper mantle beneath Southeast Asia. *Phys. Earth Planet. In.,* 154, 180-195. https://doi.org/10.1016/j.pepi.2005.09.008

Li, J. T., & Song, X. D., (2018). Tearing of Indian mantle lithosphere from high-resolution seismic images and its implications for lithosphere coupling in southern Tibet. *PNAS,* 115, 8296–8300. www.pnas.org/cgi/doi/10.1073/pnas.1717258115

Li, L., Li, A. B., Shen, Y., Sandvol, E. A., Shi, D. N., Li, H. Y., & Li, X. F. (2013). Shear wave structure in the northeastern Tibetan Plateau from Rayleigh wave tomography. *J. Geophys. Res.,* 118, 4170-4183. https://doi.org/10.1002/jgrb.50292

Li, S., van Hinsbergen, D. J. J., Deng, C., Advokaat, E. L., & Zhu, R. (2018). Paleomagnetic constraints from the Baoshan area on the deformation of the Qiangtang-Sibumasu terrane around the eastern Himalayan syntaxis. *J. Geophys. Res.*, 123, 977-997. https://doi.org/10.1002/2017JB015112

Li, Y. H., Wu, Q.J., Pan, J. T., Zhang, F. X., & Yu, D. X. (2013). An upper-mantle S-wave velocity model for East Asia from Rayleigh wave tomography. *Earth Planet. Sc. Lett.,* 377-378, 367-377. https://doi.org/10.1016/j.epsl.2013.06.033

Liang, X. F., Sandvol, E., Chen, Y. J., Hearn, T., Ni, J., Klemperer, S., Shen, Y., & Tilmann, F. (2012). A complex Tibetan upper mantle: A fragmented Indian slab and no south-verging subduction of Eurasian lithosphere. *Earth Planet. Sc. Lett.,* 333-334, 101-111. https://doi.org/10.1016/j.epsl.2012.03.036

Liang, X. F, Chen,Y., Tiana, X.B ., Chen, Y. S. J., Ni, J., Gallegos, A., Klemperer, S. L., Wang, M. L., Xu, T., Sun, C. Q., Si, S. K., Lan, H. Q. & Teng, J. W., (2016). 3D imaging of subducting and fragmenting Indian continental lithosphere beneath southern and central Tibet using body-wave finite-frequency tomography. *Earth Planet. Sc. Lett.,* 443, 162-175. https://doi.org/10.1016/j.epsl.2016.03.029

Liu, W., Li, F. Q., Yuan, S. H., Zhang, W. P., Zhuo, J. W., Wang, B. D., & Tang, W. Q. (2010). Volcanic rock provenance of Zenong Group in Coqen area of Tibet: geochemistry and Sr–Nd isotopic constraint (in Chinese with English abstract). *Acta Pertrol. Mineral.,* 29, 367-376.

Lustrino, M. (2005). How the delamination and detachment of lower crust can influence basaltic magmatism. *Earth-Sci. Rev.*, 72, 21-38. https://doi.org/10.1016/j.earscirev.2005.03.004

Maruyama, S., Santosh, M., & Zhao, D. (2007). Superplume, supercontinent, and post-perovskite: Mantle dynamics and anti-plate tectonics on the Core-Mantle Boundary. *Gondwana Res.,* 11, 7-37. https://doi.org/10.1016/j.earscirev.2010.12.002

McKenzie, D., & Priestley, K. (2016). Speculations on the formation of cratons and cratonic basins. *Earth Planet. Sci. Lett.,* 435, 94-104. https://doi:10.1016/j.gr.2008.11.004

Molnar, P., England, P., & Martinod, J. (1993). Mantle dynamics, uplift of the Tibetan Plateau and the Indian monsoon. *Rev. Geophys.,* 31, 357-396. https://doi.org/10.1016/j.resmic.2008.05.007

Molnar, P., & Tapponnier, P. (1975). The Cenozoic tectonics of Asia: effects of a continental collision. *Science,* 189, 419-426. https://doi.org/10.1126/science.189.4201.419

Nabelek, J., Hetenyi, G., Vergne, J., Sapkota, S., Kafle, B., Jiang, M., Su, H., Chen, J., Huang, B., & the Hi-CLIMB Team (2009). Underplating in the Himalaya-Tibet collision zone revealed by the Hi-CLIMB experiment. *Science,* 325, 1371-4. https://doi.org/10.1126/science.1167719

Nelson, K .D., Zhao, W. J., Brown, L. D., Kuo, J., Che, J. K., Liu, X. W., Klemperer, S. L., Makovsky, Y., Meissner, R., Mechie, J., Kind, R., Wenzel, F., Ni, J., Nabelek, J., Chen, L. S., Tan, H. D., Wei, W. B., Jones, A. G., Booker, J., Unsworth, M., Kidd, W. S. F., Hauck, M., Alsdorf, D., Ross, A., Cogan, M., Wu, C. D., Sandvol, E., & Edwards, M. (1996). Partially molten middle crust beneath southern Tibet: synthesis of project INDEPTH results. *Science,* 274, 1684-1688. https://doi.org/10.1126/science.274.5293.1684

Niu, Y. (2017). Slab breakoff: a causal mechanism or pure convenience?. *Science Bulletin,* 62, 456-461. http://dx.doi.org/10.1016/j.scib.2017.03.015

Nunn, C., Roecker, S. W., Tilmann, F. J., Priestley, K. F., Heyburn, R., Sandvol, E. A., & Team IV, T. I. (2014). Imaging the lithosphere beneath NE Ti-

bet: teleseismic P and S body wave tomography incorporating surface wave starting models. *Geophys. J. Int.*, 196(3), 1724-1741. http://creativecommons.org/licenses/by/3.0/

Paige, C., & Saunders, M. L. (1982) SQR: an algorithm for sparse linear equations and sparse least squares. *Assoc. Comput. Math. Trans. Math. Software,* 8, 43-71. https://doi.org/10.1016/j.procs.2012.04.009

Pandey, S., Yuan, X., Debayle, E., Priestley, K., Kind, R., Tilmann, F., & Li, X. (2014). A 3D shear-wave velocity model of the upper mantle beneath China and the surrounding areas. *Tectonophysics,* 633, 193-210. https://doi.org/10.1016/j.tecto.2014.07.011

Rawlinson, N., & Spakman, W. (2016). On the use of sensitivity tests in seismic tomography. *Geophys. J. Int.,* 205, 1221-243. http://creativecommons.org/licenses/by/3.0/

Rawlinson, N., Fichtner, A., Sambridge, M., & Young, M. K. (2014). Seismic tomography and the assessment of uncertainty. *Adv. Geophysic,* 55, 1-76. www.pnas.orgycgiydoiy10.1073ypnas.210382197

Replumaz, A., Capitano, F.A., Guillot, S., Negredo, M., & Villasenor, A. (2014). The coupling of Indian subduction and Asian continental tectonics. *Gondwana Res.*, 26, 608-626. https://doi.org/10.1016/j.gr.2014.04.003

Replumaz, A., Guillot, S., Villasenor, A., & Negredo, A. M. (2013). Amount of Asian lithospheric mantle subducted during the India/Asia collision. *Gondwana Res.,* 24, 936-945. https://doi.org/10.1016/j.gr.2012.07.019

Roger, F., Tapponnier, P., Arnaud, N., Schärer, U., Brunel, M., Xu, Z., & Yang, J. (2000). An Eocene magmatic belt across central Tibet: mantle subduction triggered by the Indian collision?. *Terra Nova,* 12, 102-108. https://doi.org/10.1046/j.1365-3121.2000.123282.x

Royden, L .H., Burchfiel, B. C., & van der Hilst, R. D. (2008). The geological evolution of the Tibetan plateau. *Science,* 321, 1054-1058. https://doi.org/10.1126/science.1155371

Schmandt, B., Jacobsen, S. D., Becker, T. W., Liu, Z., & Dueker, K. G. (2014). Dehydration melting at the top of the lower mantle. *Science,* 344. https://doi.org/10.1126/science.12533581265-1268

Schulte-Pelkum, V., Monsalve, G., Sheehan, A., Pandey, M. R., Sapkota, S., Bilham, R., & Wu, F., (2005). Imaging the Indian subcontinent beneath the Himalaya. *Nature,* 435, 1222-1225. https://doi.org/0.1038/nature03678

Sol, S., Meltzer, A., Burgmann, R., van der Hilst, R. D., King, R., Chen, Z., Koons, P. O., Lev, E., Liu, Y. P., Zeitler, P. K., Zhang, X., Zhang, J., & Zurek, B. (2007). Geodynamics of the southern Tibetan Plateau from seismic anisotropy and geodesy. *Geology,* 35, 563-566. https://doi.org/10.1130/G23408A.1; 3

Stern, C. R., & Kilian, R. (1996). Role of the subducted slab, mantle wedge and continental crust in the generation of adakites from the

Andean Austral volcanic zone. Contrib. *Mineral. Petr.,* 123, 263-281. https://doi.org/10.1007/s004100050155

Sui, Q. L., Wang, Q., Zhu, D. C., Zhao, Z. D., Chen, Y., Santosh, M., Hu, Z. C., Yuan, H. L., & Mo, X. X. (2013). Compositional diversity of ca. 110 Ma magmatismin the northern Lhasa Terrane, Tibet: Implications for the magmatic origin and crustal growth in a continent–continent collision zone. *Lithos,* 168-169, 144-159. https://doi.org/10.1016/j.lithos.2013.01.012

Sun, Y. J., Dong, S. W., Zhang, H., Li, H., & Shi, Y. L. (2013). 3D thermal structure of the continental lithosphere beneath China and adjacent regions. *J Asian Earth Sci.,* 62, 697-704. http://dx.doi.org/10.1016/j.jseaes.2012.11.020

Tapponnier, P., Xu, Z. Francüoise, R., Bertrand, M., Nicolas, A., Gérard, W., & Yang, J. (2001). Oblique Stepwise Rise and Growth of the Tibet Plateau. *Science,* 294, 1671-1677. https://doi.org/10.1126/science.105978

Toksoz, M. N., & Bird, P. (1977). Island Arcs, Deep Sea Trenches and Back-Arc Basins (ed. Talwani, M., Pitman, W. C.) 379-393 (American Geophysical Union, Washington, D.C.).

Turner, S., Arnaud, N., Liu, J., Rogers, N., Hawkesworth, C., Harris, N., Kelley, S., van Calsteren, P., & Deng, W.M. (1996). Postcollisional, shoshonitic volcanism on the Tibetan plateau: implications for convective thinning of the lithosphere and the source of ocean island basalts. *J. Petrol.,* 37, 45-71. https://doi.org/10.1093/petrology/37.1.45

Unsworth, M., Wei, W., Jones, A. G., Li, S., Bedrosian, P., Booker, J., Jin, S., Deng, M. & Tan, H., (2004). Crustal and upper mantle structure of northern Tibet imaged with magnetotelluric data. *J. Geophys. Res.,* 109, B02403. https://doi.org/10.1029/2002JB002305

Vozar, J., Jones, A. G., Fullea, J., Agius, M. R., Lebedev, S., Le Pape, F., & Wei, W. (2014). Integrated geophysical-petrological modeling of lithosphere-asthenosphere boundary in central Tibet using electromagnetic and seismic data. *Geochemistry, Geophysics, Geosystems*, 15(10), 3965-3988. https://doi.org/doi:10.1002/2014GC005365

Wang, X. C., Li, Z. X., Li, X. H., Li, J., Xu, Y. G., & Li, X. H. (2013). Identification of an ancient mantle reservoir and young recycled materials in the source region of a young mantle plume: Implications for potential linkages between plume and plate tectonics. *Earth Planet. Sc. Lett.,* 377-378, 248-259. https://doi.org/10.1016/j.epsl.2013.07.003

Wei, W. B., Unsworth, M., Jones, A., Booker, J., Tan, H. D., Nelson, D., Chen, L. S., Li, S. H., Solon, K., Bedrosian, P., Jin, S., Deng, M., Ledo, J., Ray, D., & Roberts, B. (2001). Detection of widespread fluids in the Tibetan crust by magnetotelluric studies. *Science,* 292, 716-718. https://doi.org/10.1126/science.1010580

Williams, H. M., Turner, S. P., Pearce, J. A., Kelley, S. P., & Harris, N. B. W. (2004). Nature of the source regions for post-collisional, potassic magmatism

in southern and northern Tibet from geochemical variations and inverse trace element modelling. *J. Petrol.,* 45, 555-607. https://doi.org/10.1093/petrology/egg094

Wortel, M. J. R., & Spakman, W. (1992). Structure and dynamics of subducted lithosphere in the Mediterranean region. *Proc. K. Ned. Akad. Wet.,* 95, 325-347.

Xiao, Z., Fuji, N., Iidaka, T., Gao, Y., Sun, X., & liu, Q. (2020). Seismic structure beneath the Tibetan Plateau from iterative finite-frequency tomography based on ChinArray: New insights into the Indo-Asian collision. *J. Geophys. Res.*, 125, e2019JB018344. https://doi.org/10.1029/2019JB018344

Xu, Q., Zhao, J. M., Pei, S .P., & Liu, H. B. (2011). The lithosphere–asthenosphere boundary revealed by S-receiver functions from the Hi-CLIMB experiment. *Geophys. J. Int.,* 187, 414-420. https://doi.org/10.1111/j.1365-246X.2011.05154.x

Xu, Q., Zhao, J. M., Yuan, X. H., Liu, H. B., & Pei, S. P. (2015). Mapping crustal structure beneath southern Tibet: Seismic evidence for continental crustal underthrusting. *Gondwana Res.*, 27, 1487-1493. https://doi.org/10.1016/j.gr.2014.01.006

Yang, Y.J., Ritzwoller, M. H., Zheng, Y., Shen, W. S., Levshin, A .L., & Xie, Z. J. (2012). A synoptic view of the distribution and connectivity of the mid-crustal low velocity zone beneath Tibet. *J. Geophys. Res.*, 117, B04303. https://doi.org/10.1029/2011JB008810

Yin, A., Harrison, T. M. (2000). Geologic evolution of the Himalayan–Tibetan orogen. *Ann. Rev. Earth Planet. Sci.,* 28, 211-280. https://doi.org/10.1146/annurev.earth.28.1.211

Yuan, X. H., Ni, J., Kind, R., Mechie, J., & Sandvol, E. (1997). Lithospheric and upper mantle structure of southern Tibet from a seismological passive source experiment. *J. Geophys. Res.,* 102, 27491-27500. https://doi.org/10.1029/97JB02379

Zhang, H., Zhao, D., Zhao, J. M., & Liu, H. B. (2015). Tomographic imaging of the underthrusting Indian slab andmantle upwelling beneath central Tibet. *Gondwana Res.,* 28, 121-132. https://doi.org/10.1016/j.gr.2014.02.012

Zhao, D., Hasegawa, A., & Horiuchi, S. (1992). Tomographic imaging of P- and S-wave velocity structure beneath northeastern Japan. *J. Geophys. Res.,* 97, 19909-19928, https://doi.org/10.1029/92JB00603

Zhao, D., Hasegawa, A., & Kanamori, H. (1994). Deep structure of Japan subduction zone as derived from local, regional and teleseismic events. *J. Geophys. Res.,* 99, 22313-22329. https://doi.org/10.1029/94JB01149

Zhao, J., Yuan, X. H., Liu, H. B, Kumar, P., Pei, S. P., Kind, R., & Zhang, Z. J., (2010). The boundary between the Indian and Asian tectonic plates below Tibet. *PNAS*, 107(25), 11,229-11,233. doi:10.1073/ pnas.1001921107

Zhao, Z. D., Mo, X. X., Dilek, Y., Niu, Y. L., DePaolo, D. J., Robinson, P., Zhu, D. C., Sun, C. G., Dong, G. C., Zhou, S., Luo, Z. H., & Hou, Z. Q. (2009). Geochemical and Sr-Nd-Pb-O isotopic compositions of the post-collisional ultrapotassic magmatism in SW Tibet: petrogenesis and implications for India intra-continental subduction beneath southern Tibet. *Lithos,* 113, 190-212. https://doi:10.1016/j.lithos.2010.02.014

Zheng, X. F., Yao, Z. X., Liang, J. H., & Zheng, J. (2010). The Role Played and Opportunities Provided by IGP DMC of China National Seismic Network in Wenchuan Earthquake Disaster Relief and Researches. *Bull. Seis. Soc. Am.,* 100, 2866-2872. https://doi.org/10.1785/0120090257

Zhu, D. C., Mo, X. X., Niu, Y. L., & Zhao, Z. D. (2009). Geochemical investigation of Early Cretaceous igneous rocks along an east–west traverse throughout the central Lhasa Terrane. Tibet. *Chem. Geol.,* 268, 298-312. https://doi.org/10.1016/j.chemgeo.2009.09.008

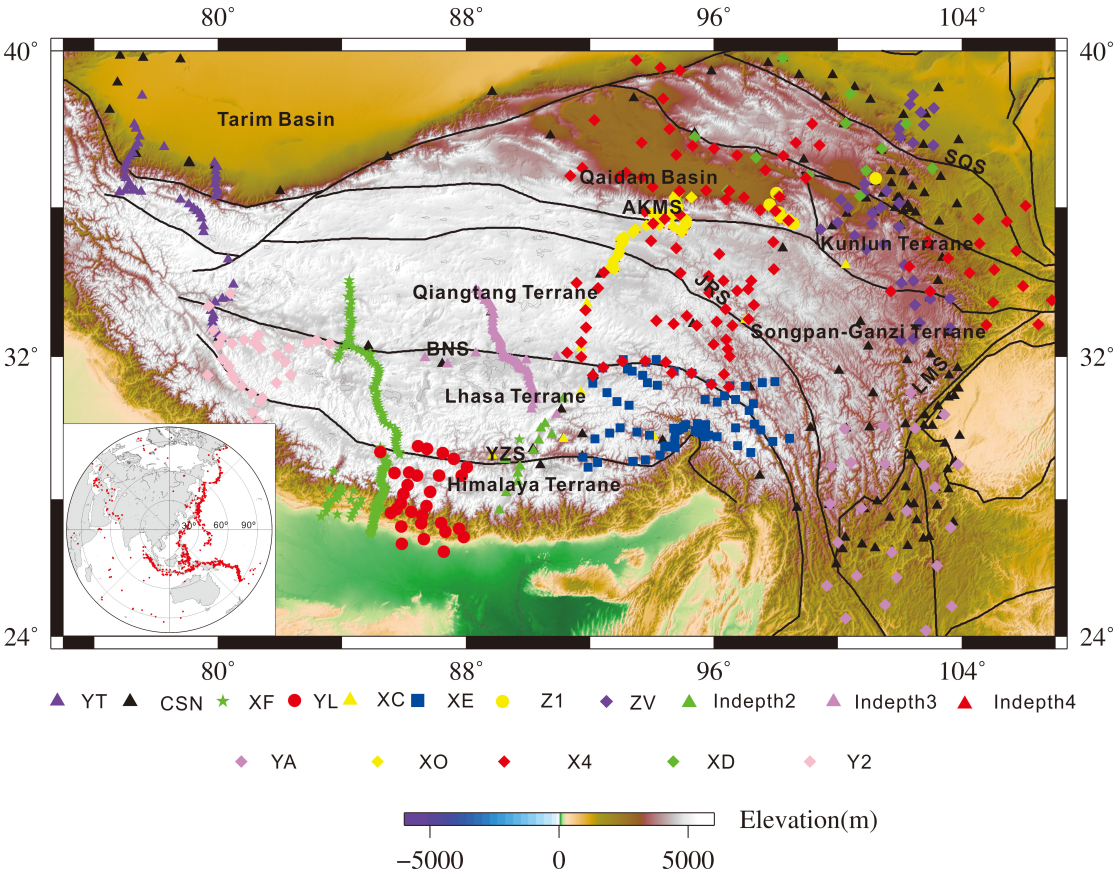

Fig. 1 Tectonic framework of the Tibetan region and distribution of seismic stations. Indus–Yarlung suture: YZS, Bangong–Nujiang suture: BNS, Jinshajiang

suture: JRS, Anyimaqen–Kunlun–Mutztagh suture: AKMS, and South Qilian suture: SQS. CSN: permanent seismic station recorded by the China seismic network.

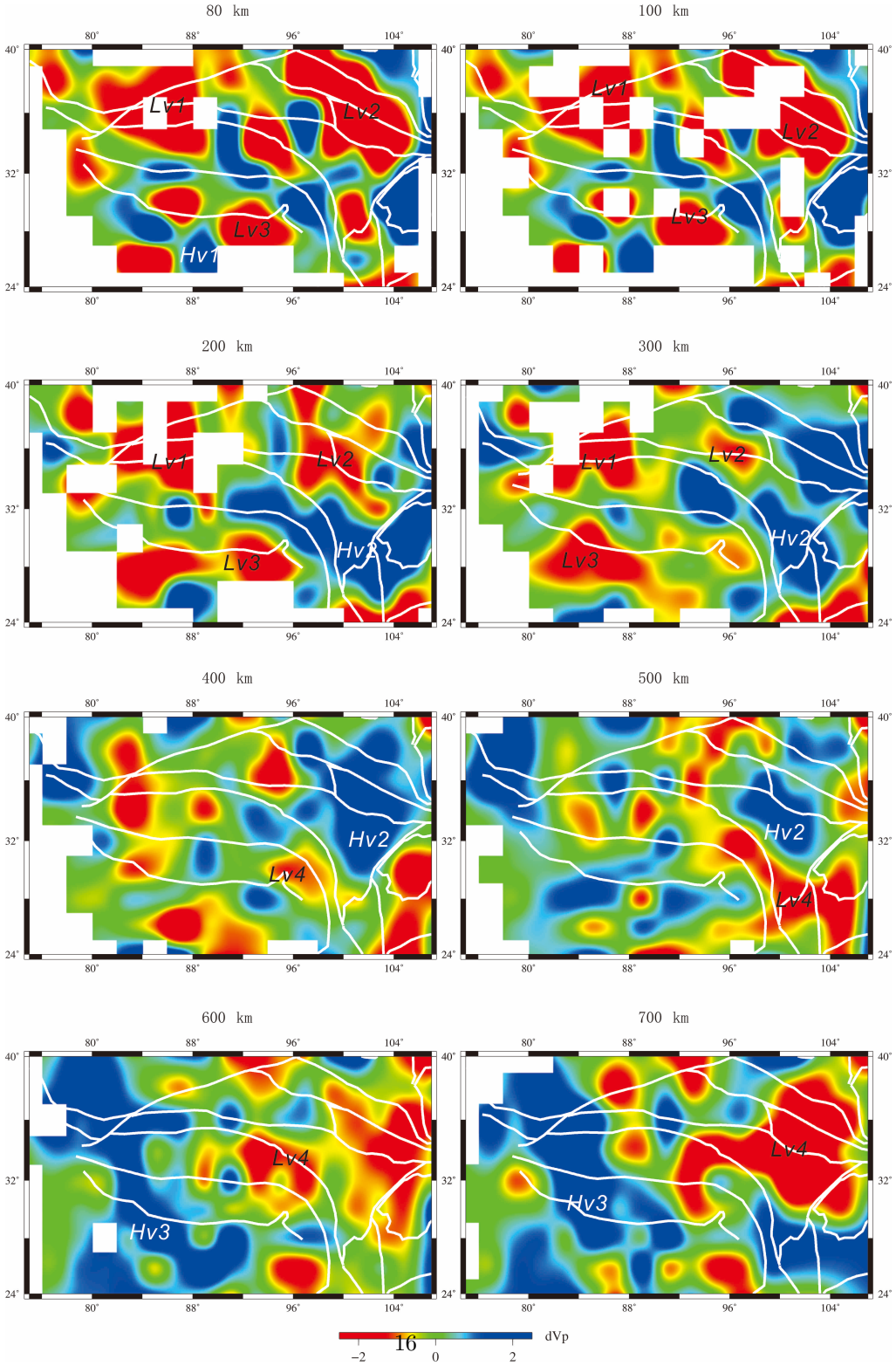
80 km
100 km
200 km
300 km
400 km
500 km
600 km
700 km
Lv1
Lv2
Lv3
Hv1
Hv2
Hv3
Lv4
80°
88°
96°
104°
40°
32°
24°
−2
0
2
dVp

Fig. 2 P-wave velocity perturbations at depths of 80, 100, 200, 300, 400, 500, 600 and 700 km relative to the IASP91 1-D velocity model (Kennett & Engdahl, 1991). Portions of the model where the recovery of the starting model in the CRT was below 10% are not shown (see Fig. S2).

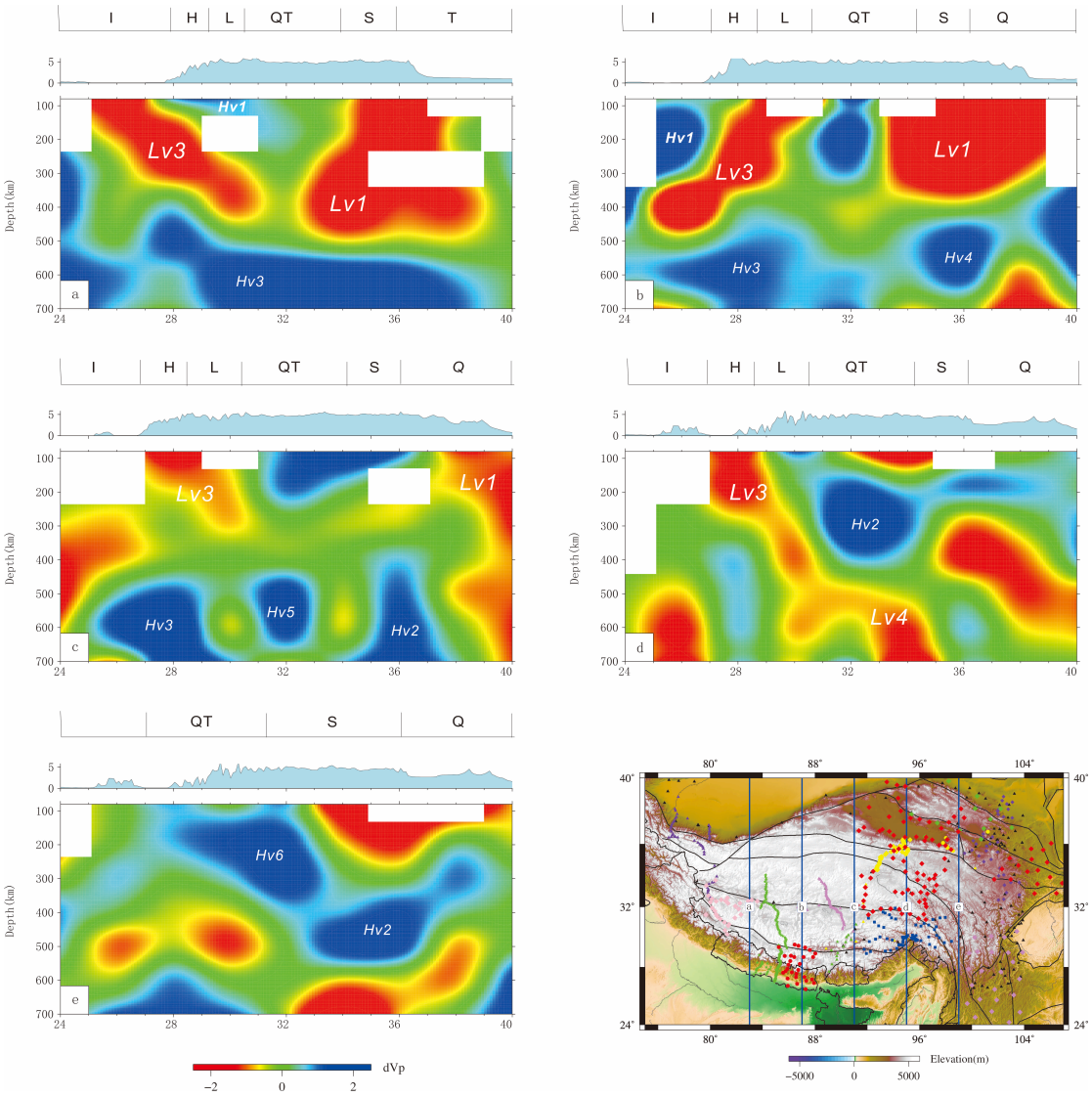

Fig. 3 Longitudinal profiles. I: Indian plate, H: Himalaya terrane, QT: Qiangtang terrane, S: Songpan-Ganzi terrane, Q: Qaidam terrane, T: Tarim Basin. Portions of the model where the recovery of the starting model in the CRT was below 10% are not shown (Fig. S8). Horizontal coordinate: latitude (degree).

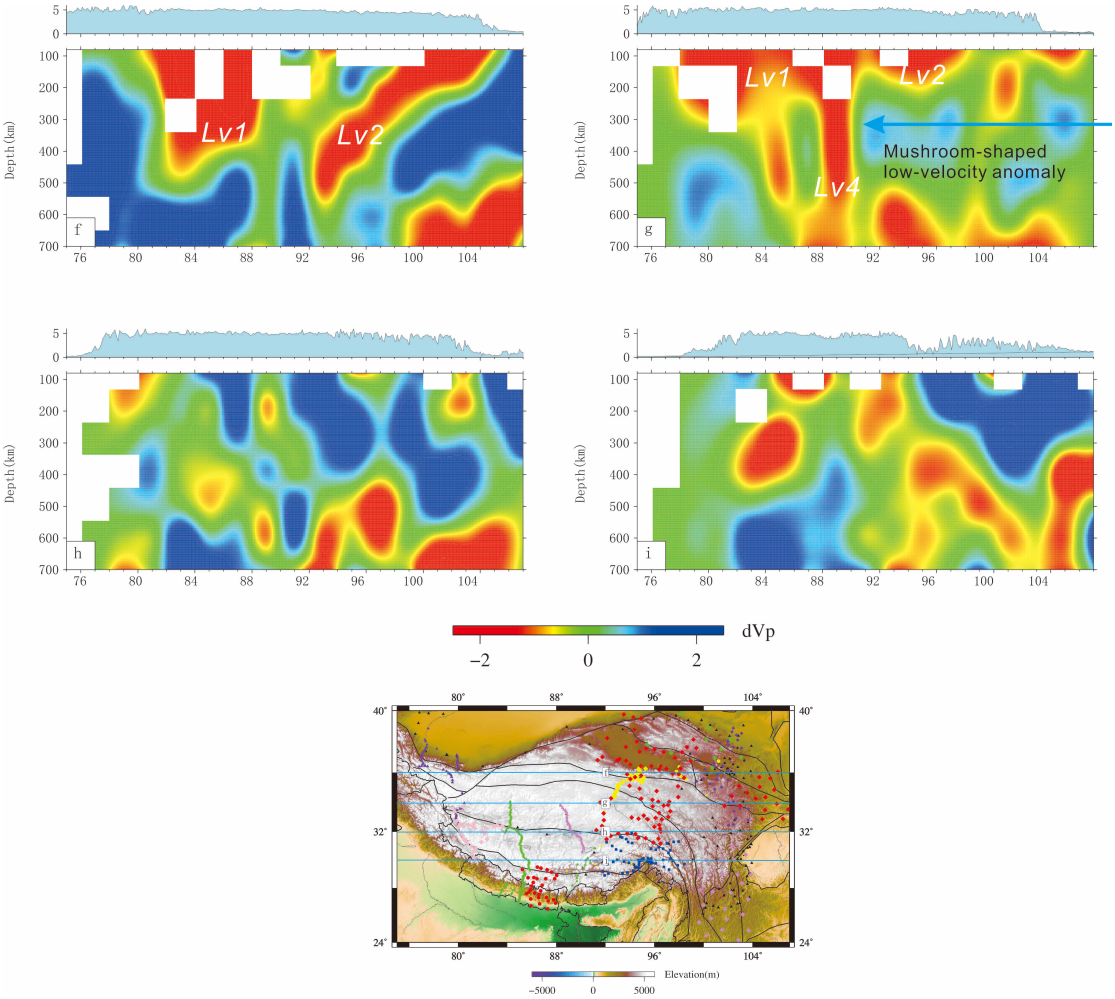

Fig. 4 Latitudinal profiles. Portions of the model where the recovery of the starting model in the CRT was below 10% are not shown (Fig. S9). Horizontal coordinate: longitude (degree).

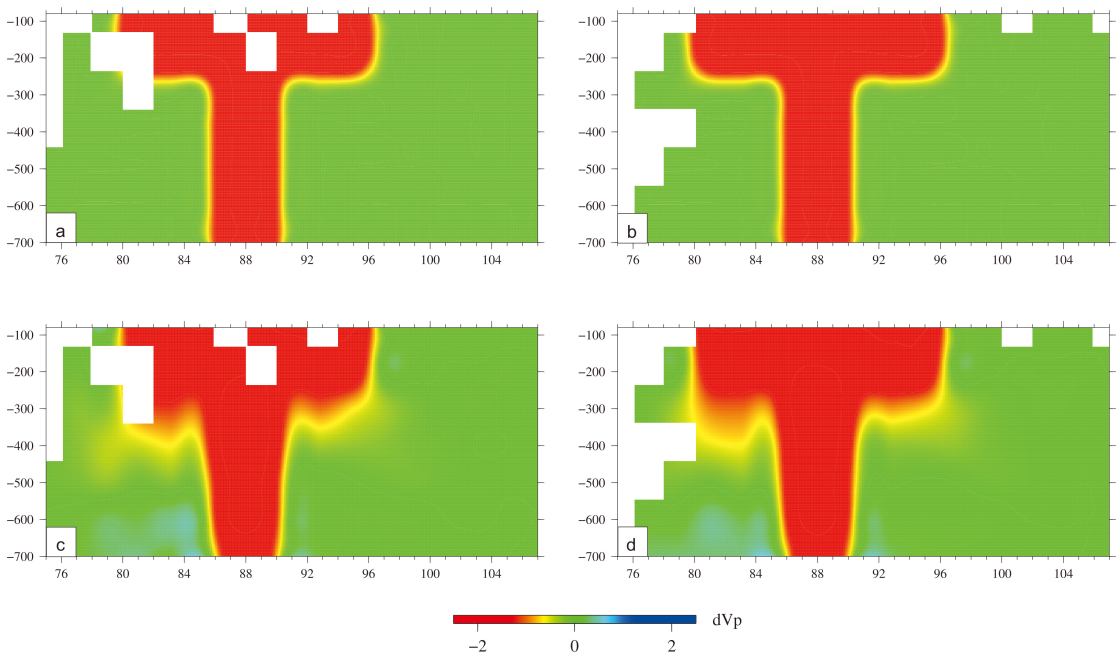

Fig. 5 Synthetic tests a and b are input models along the 34° and 32° profiles (profile location, see Fig. 4, b and c profiles), respectively; c and d are output models along the 34° and 32° profiles (profile location, see Fig. 4), respectively. The portions of the model where the recovery of the starting model in the CRT was below 10% are not shown (see Fig. S9). The test results show that the major low-velocity anomaly (Lv1) of the output model reflects that of the input model.